SYNTHESIS, CHARACTERIZATION, AND APPLICATION OF MANGANESE-DOPED IRON SULFIDE NANOPLATELETS ON CARBON CLOTH: A NEGATIVE FLEXIBLE AND WEARABLE ELECTRODE MATERIAL FOR FUTURE ELECTRONICS AND ENERGY STORAGE

A THESIS SUBMITTED TO
THE GRADUATE SCHOOL OF NATURAL AND APPLIED SCIENCES
OF
MIDDLE EAST TECHNICAL UNIVERSITY

BY

ALMİLA NUR GÖZÜTOK

IN PARTIAL FULFILLMENT OF THE REQUIREMENTS
FOR
THE DEGREE OF MASTER OF SCIENCE
IN
CHEMISTRY

SEPTEMBER 2023

Approval of the thesis:

SYNTHESIS, CHARACTERIZATION, AND APPLICATION OF MANGANESE-DOPED IRON SULFIDE NANOPLATELETS ON CARBON CLOTH: A NEGATIVE FLEXIBLE AND WEARABLE ELECTRODE MATERIAL FOR FUTURE ELECTRONICS AND ENERGY STORAGE

submitted by **ALMİLA NUR GÖZÜTOK** in partial fulfillment of the requirements for the degree of **Master of Science** i**n Chemistry, Middle East Technical University** by,

Prof. Dr. Halil Kalıpçılar
Dean, Graduate School of **Natural and Applied Sciences** _____

Prof. Dr. Özdemir Doğan
Head of the Department, **Chemistry** _____

Prof. Dr. Emren Nalbant
Supervisor, **Chemistry, METU** _____

Examining Committee Members:

Prof. Dr. Ayşen Yılmaz
Chemistry, METU _____

Prof. Dr. Emren Nalbant
Chemistry, METU _____

Prof. Dr. Hüsnü Emrah Ünalan
Metallurgical and Materials Eng., METU _____

Assoc. Prof. Dr. Oktay Demircan
Chemistry, Boğaziçi Uni. _____

Asist. Prof. Dr. Demet Asil Alptekin
Chemistry, METU _____

Date: 06.09.2023

I hereby declare that all information in this document has been obtained and presented in accordance with academic rules and ethical conduct. I also declare that, as required by these rules and conduct, I have fully cited and referenced all material and results that are not original to this work.

Name Last name: Almila Nur Gözütok

Signature:

ABSTRACT

SYNTHESIS, CHARACTERIZATION, AND APPLICATION OF MANGANESE-DOPED IRON SULFIDE NANOPLATELETS ON CARBON CLOTH: A NEGATIVE FLEXIBLE AND WEARABLE ELECTRODE MATERIAL FOR FUTURE ELECTRONICS AND ENERGY STORAGE

Gözütok, Almila Nur
Master of Science, Chemistry
Supervisor: Prof. Dr. Emren Nalbant

September 2023, 53 pages

Addressing the urgent need for eco-friendly solutions in capturing and storing clean energy has prompted a search for efficient alternatives. As society becomes more mobile and demands flexible, compact, and highly efficient future electronics, exploring new materials that meet these criteria is crucial. This thesis is motivated by the idea of harnessing the potential of manganese-iron-sulfur-based electrodes, an intriguing yet underused material, by directly growing them on carbon cloths to create flexible electrode materials for energy storage applications. The hydrothermal method was strategically selected for manufacturing these electrodes, as it enhances the interaction between the active material and the entire 3D network of the textile while overcoming challenges associated with synthetic methods and insulating binders. Through thorough evaluations of electrochemical performance, this study aims to determine the viability of fabricated electrodes as promising candidates for future electronics, and the results have been highly encouraging. The thesis includes various studies, such as the successful direct growth of nanoparticles on carbon cloth,

morphological and structural characterizations of as-synthesized material using multiple analytical methods, preparation of negative and positive electrodes to construct a flexible device, and detailed electrochemical characterization and investigation of the application potential of the as-prepared electrodes for real-world scenarios. The prepared electrodes demonstrated remarkable performance, exhibiting a high specific capacitance of 206 F g^{-1} and exceptional cyclic stability up to 11000 cycles. Moreover, by employing a specialized encapsulation technique, the as-fabricated electrodes exhibited efficient operation over an extended period of three months. These electrodes were then integrated to create a self-powered flexible supercapacitor, successfully illuminating embedded green LED arrays within a hoodie.

Keywords: Flexible Supercapacitors, Negative Electrodes, Energy Storage, Supercapacitors, Transition-metal-sulfides

ÖZ

GELECEĞİN ELEKTRONİKLERİ VE ENERJİ DEPOLAMA SİSTEMLERİ İÇİN ESNEK VE GİYİLEBİLİR NEGATİF ELEKTROT MALZEMESİ OLARAK MANGANEZ KATKILI DEMİR SÜLFÜRLERİN KARBON KUMAŞLAR ÜZERİNDE SENTEZİ, KARAKTERİZASYONU VE UYGULAMASI

Gözütok, Almila Nur
Yüksek Lisans, Kimya
Tez Yöneticisi: Prof. Dr. Emren Nalbant

Eylül 2023, 53 sayfa

Temiz enerjiyi yakalama ve depolamada çevre dostu çözümlere olan acil ihtiyaca yanıt olarak, etkili alternatiflerin arayışı önem kazanmıştır. Toplumumuzun giderek daha hareketli hale gelmesi ve esnek, kompakt ve son derece verimli gelecek elektroniklere olan talebin artmasıyla, bu gereksinimleri karşılayabilecek yeni malzemeleri keşfetmek hayati hale gelmiştir. Bu tez, ilgi çekici fakat literatürde yeterince kullanılmamış bir malzeme olan manganez-demir-kükürt bazlı elektrotların potansiyelini, doğrudan karbon kumaşlar üzerinde büyüterek enerji depolama uygulamaları için esnek elektrot malzemeleri oluşturma fikrine dayanmaktadır. Bu elektrotların imalatı için hidrotermal yöntem stratejik olarak seçilmiştir, çünkü aktif malzeme ile tekstilin tüm 3D ağı arasındaki etkileşimi maksimize ederken sentetik yöntemlerle ve yalıtkan bağlayıcıların kullanımı ile ilişkili zorlukları aşmaktadır. Kapsamlı elektrokimyasal performans değerlendirmeleri aracılığıyla, bu çalışma nanomalzemenin gelecekteki elektronikler için umut vaat eden adaylar olarak uygunluğunu belirlemeyi amaçlamaktadır ve şimdiye kadar elde edilen sonuçlar son derece cesaret vericidir. Bu tez,

nanoparçacıkların karbon kumaş üzerinde doğrudan büyümesi, farklı analitik yöntemlerle morfolojik ve yapısal karakterizasyonları, esnek bir cihaz oluşturmak için negatif ve pozitif elektrotların hazırlanması ve hazırlanan elektrotların gerçek dünya senaryoları için elektrokimyasal karakterizasyonu ve uygulama potansiyelinin araştırılması gibi çeşitli çalışmaları içermektedir. Hazırlanan elektrotlar, yüksek özgül kapasitansıyla (206 F g^{-1}) ve olağanüstü döngüsel stabilitesiyle (11000 döngüye kadar) dikkat çekici performans sergilemiştir. Ayrıca, üretilen elektrotlar, üç aya kadar verimli çalışmayı sağlayacak şekilde özel bir kapsülleme tekniği kullanılarak kaplanmıştır. Bu elektrotlar daha sonra bir araya getirilerek esnek ve giyilebilir elektronik cihazlar için tasarlanmış, kendi enerjisini üreten bir süperkapasitör oluşturulmuş ve hoodie içine gömülü yeşil LED dizilerini aydınlatmak için başarıyla kullanılmıştır. Bu önemli çalışma, esnek ve giyilebilir elektronik cihazlar için pratik uygulamalarda büyük umut vadetmektedir.

Anahtar Kelimeler: Esnek Süperkapasitörler, Negatif Elektrotlar, Enerji Depolama, Süperkapasitörler, Geçiş-metal-sülfürleri

"Though fairy tales end after ten pages, our lives do not. We are multi-volume sets. In our lives, even though one episode amounts to a crash and burn, another episode is always awaiting us, and then another. There are always more opportunities to get it right, to fashion our lives in the ways we deserve to have them. Don't waste your time hating a failure. Failure is a greater teacher than success."

Clarissa Pinkola Estés, Woman Who Run with the Wolves (1989)

To my beloved father,

May we meet again

ACKNOWLEDGMENTS

I want to express my heartfelt gratitude to my supervisor, Professor Dr. Emren Nalbant, for being there for me during my most challenging moments and never giving up on me. Thank you for mentoring me and being like an older sister, showing unwavering belief in me, and providing unwavering support. Thank you for opening a whole new world of possibilities and for your constant support and trust. I wish for your beautiful laughter to always fill the air with happiness.

I would like to sincerely thank Prof. Dr. Hüsnü Emrah Ünalan for believing in me and guiding this project to heights I never thought possible. I am delighted to have experienced his great sense of humor and the warmth of his kind and welcoming heart, even though his outer demeanor may seem strict. I wish him a life filled with success and happiness, as he truly deserves it.

I am thrilled to have embarked on this journey with my 'Gandalf,' Dr. Mete Batuhan Durukan. This research would never have been possible without him. I am immensely grateful to him for sharing his excitement for knowledge and expanding my horizons with all the wisdom he imparted to me. Thank you a thousand times over. Now, 'I shall pass' because of him.

I would like to express my sincere gratitude to Prof. Dr. Emrah Özensoy, Dr. Yusuf Koçak, and members of the Ozensoy Research Group for their invaluable guidance and expertise in conducting X-ray photoelectron spectroscopy (XPS) measurements and analysis for this study. Their profound knowledge of XPS instrumentation, experimental setup, and data interpretation significantly contributed to the accuracy and reliability of the results.

My heartfelt gratitude goes out to all my friends, including Serkan Alantor, Deniz Barun, Umut Bolatbaş, Başak Burçak Demir, Gizem Gökdemir, Duygu Gümüş, Ceren Kaplan, Deniz Keskin, Anas Khaled, Baturalp Olgun, Ayşe Yıldırım and

countless others whom I can't name due to the character limit. Being surrounded by each one of you in this beautiful journey brings an indescribable warmth to my heart. I am beyond grateful for the laughter, support, and unforgettable memories we've shared. As we navigate through life's playground hand in hand, I eagerly await the boundless moments of happiness and togetherness that lie ahead.

And Abdullah Güçlü, thank you for being my 'Appa.' Your amazing character and heart of gold fill my heart with profound gratitude. Knowing that there are still individuals like you in this world restores my faith in humanity. Thank you from the depths of my soul for being by my side through the ups and downs, sharing my laughter, and wiping away my tears. I love you wholeheartedly.

And most importantly, to my wonderful sister, Ahu Gözütok, and my dear mother, Ayfer Gültekin, I want to thank you from the bottom of my heart for being there for me when I needed it the most. Ahu, your unique sense of humor and jokes have helped me feel better when going through tough times and having an existential crisis. Your funny and playful ways brought a lot of joy and light to my life. And Mom, your positive attitude towards life has been a great support to me. Your love and encouragement have given me strength and hope during difficult moments. With both of you by my side, I feel strong and capable of handling anything. I am grateful for the comfort and love you've shown me, and I will always cherish our bond.

I want to express my sincere appreciation to everyone who has played a role in shaping my thesis journey. To my dear lab friends, the dedicated department staff, and the esteemed professors who generously shared their ideas, I am deeply thankful.

This work is partially funded by the Bilimsel Araştırma Projeleri Koordinasyon Birimi under grant number TEZ-YL-103-2022-10906.

TABLE OF CONTENTS

LIST OF TABLES

LIST OF FIGURES

FIGURES

LIST OF ABBREVIATIONS

ABBREVIATIONS

AC	Activated Carbon
CC	Carbon Cloth
CNT	Carbon Nanotube
CV	Cyclic Voltammetry
EC	Electrochemical Capacitor
EDLC	Electric Double Layer Capacitor
EDX	Energy Dispersive X-Ray
EIS	Electrochemical Impedance Spectroscopy
ESR	Equivalent Series Resistance
GCD	Galvanostatic Charge Discharge
MFS	Manganese Doped Iron Sulfide
MS	Manganese Sulfide
MFS-CC	Manganese Doped Iron Sulfide on Carbon Cloth
MS-CC	Manganese Sulfide on Carbon Cloth
rGO	Reduced Graphene Oxide
SC	Supercapacitor
SEM	Scanning Electron Microscopy
TEM	Transmission Electron Microscopy
XPS	X-Ray Photoelectron Spectroscopy
XRD	X-Ray Diffraction

CHAPTER 1

INTRODUCTION

1.1 Motivation for the Study

The quest for efficient alternatives has become paramount in response to the pressing need for environmentally benign solutions in capturing and storing clean energy. As our society becomes increasingly mobile and the demand for flexible, compact, and highly efficient future electronics increases, it becomes imperative to explore novel materials that meet these requirements.

In recent times, there has been a growing interest in the rapid advancement of wearable electronics, including devices like bio-monitoring tools, military equipment, electric sensors, smartwatches, eyewear technology, and displays [1]. Among these, flexible supercapacitors have gained significant attention as a power source for wearable electronics due to their advantages, such as high-power output, extended lifespan, quick charging/discharging abilities, wide availability, safety, and cost-effectiveness. These attributes give them an edge over lithium-ion battery technologies [2,3]. Nevertheless, supercapacitors' relatively low energy density poses a fundamental constraint on their applicability in various industries. To address this limitation and elevate the energy density of future wearable devices, extensive research has focused on transition metal sulfides/oxides as promising electrode materials [4,5].

This thesis is driven by the compelling idea of harnessing the potential of manganese-iron-sulfur-based flexible negative electrodes, an intriguing yet underutilized material in the literature, by directly growing them on carbon cloths to create flexible electrode materials for energy storage applications. The hydrothermal

method was strategically chosen for manufacturing these electrodes, as it maximizes the interaction between the active material and the entire 3D network of the textile while circumventing the challenges associated with synthetic methods and the incorporation of insulating organic binders. Through comprehensive electrochemical performance evaluations, this study seeks to ascertain the viability of the fabricated negative electrode as a promising candidate for future electronics, and the results obtained so far have been highly encouraging. The studies encompassed in this thesis include:

- Direct growth of nanoparticles on carbon cloth successfully,
- Morphological and structural characterizations of as-synthesized material using a variety of analytical methods,
- Preparation of a negative electrode and a positive electrode to construct a flexible device,
- Electrochemical characterization of the as-prepared electrodes by two and three-electrode cell configurations,
- Electrochemical characterization and investigation of the application potential of the as-prepared electrodes for real-world scenarios.

1.2 An Overview of Electrochemical Capacitors and Their Current Status

Since the Industrial Revolution, human civilization has advanced at a breakneck pace, causing energy shortages and environmental damage. As a result, the search for sustainable and environmentally friendly energy sources has become crucial due to the depletion of fossil fuel resources and ecological problems. Following that, a need to store sustainable energy has emerged due to the increased usage of renewable energy sources like wind and solar power. In the last few decades, electrochemical energy storage systems have received much interest, and researchers have been working to develop efficient and effective storage devices. During this process,

supercapacitors (SCs) have appeared on the scene as a promising alternative due to their high power density, rate capability, and long-term cycle stability [5,6].

In 1957, a General Electric employee, Howard Becker, obtained the first patent for an electrical double-layer capacitor, employing sulfuric acid as the electrolyte and a porous carbon electrode [7]. In the following decades, significant advancements were made in supercapacitors, building upon Howard Becker's pioneering work. Researchers and engineers focused on improving these devices' energy storage capacity, efficiency, and safety. Throughout the years, efforts were directed toward developing new electrode materials to enhance the capacitance and charge-discharge rates. Introducing activated carbon and other nanostructured materials as electrodes substantially increased the surface area, improving the double-layer capacitance and leading to a surge in supercapacitor performance. The early 2000s witnessed a growing interest in asymmetric supercapacitors, combining the characteristics of traditional supercapacitors and batteries. As the demand for more sustainable and efficient energy storage solutions increased, researchers explored alternative materials like graphene, conducting polymers, and transition metal oxides, aiming further to optimize supercapacitors' specific capacitance and energy density.

The numerous shortcomings of other commercial energy storage technologies are complemented by electrochemical capacitors (ECs), which bridge the gap between conventional supercapacitors and batteries. ECs can produce greater power densities than batteries and fuel cells and higher energy densities than traditional capacitors [3]. Moreover, they undergo significantly fewer chemical phase changes when continuously charged and discharged, giving them a much longer cycle life than batteries [4]. These crucial characteristics make supercapacitors more desirable and versatile as high-powered energy storage systems, which has, in return, sparked much interest in both academic and industrial areas. Despite its rapid development, this technology still suffers from low energy density issues. To address this issue, industries and academic institutions worldwide are now striving to develop novel

and highly effective electrode and electrolyte materials for supercapacitor applications.

1.3 Electrochemical Capacitors Based on Their Charge Storage Mechanisms

Three distinct categories emerge according to their charge storage mechanisms: Electric Double-Layer Capacitors (EDLCs), Pseudocapacitors, and Hybrid Capacitors. These classifications arise due to variations in the charge storage processes, which consequently influence parameters such as energy density, capacitance, and charge/discharge kinetics.

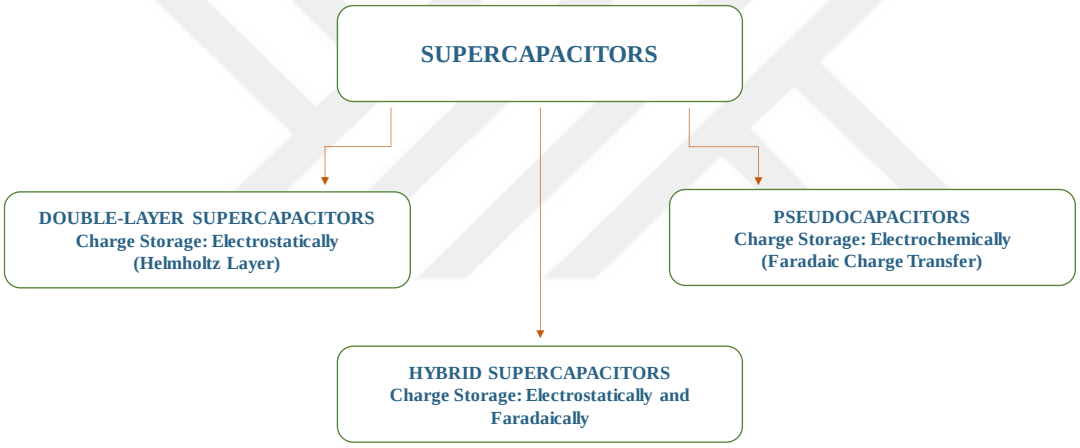

Figure 1-1 Type of supercapacitors based on their charge storage mechanisms

1.3.1 Electrical Double-Layer Supercapacitors

The charge storage mechanism of electrical double-layer capacitors (EDLCs) is based on the physical accumulation of charges at the electrode/electrolyte interfaces without electrochemical reaction at the electrode surface [2]. When voltage is applied, charge separation occurs at the electrode/electrolyte interface, creating a double layer according to the way Helmholtz described as [8]

$$C = \varepsilon_0 \varepsilon_r A/d$$

where ε_r represents the electrolyte dielectric constant, ε_0 represents the dielectric constant of the vacuum, A is the electrode surface area, and d is the distance between ions of the electrolyte and electrode. The surface area and pore-size distribution of the electrode materials significantly impact the capacitance of EDLCs. In this context, researchers widely investigated materials with conductivity and large surface areas, such as activated carbon, graphenes, and carbon nanotubes [9].

In EDLCs, when a voltage is applied, electrons migrate from the negative electrode to the positive electrode through the external loop during the charging process, leading anions of the electrolyte to move positive electrodes and cations of the electrode to negative electrodes [10,11]. Although the charge storing mechanism is Non-Faradaic in nature, leading to fast charge/discharge rates, exceptional mechanical stability, and rapid response to voltage changes, EDLCs suffer from lower energy densities, preventing them from being efficient supercapacitor-type energy storage materials and need further developments.

1.4 Pseudocapacitors

Pseudocapacitors are electrochemical capacitors that store charge through fast and reversible faradaic redox reactions at the electrode-electrolyte interface. These reactions involve the transfer of electrons, leading to changes in the oxidation state of the electrode material, which allows for higher energy storage capabilities compared to traditional capacitors (EDLCs).

The term "pseudocapacitance" was derived from "pseudocapacity," a term introduced by David C. Grahame in 1941 and later expanded upon by John B. Conway in 1991 [12,13]. Conway used the word "pseudocapacitance" to differentiate this specific type of capacitor from the more common EDLC-type capacitors, which rely on non-faradaic physical charge storage at the electrode-electrolyte interface.

Pseudocapacitors hold immense potential for energy storage applications because the faradaic redox processes allow for rapid charge and discharge rates, resulting in higher power densities than EDLCs.

1.5 Hybrid Supercapacitors

Hybrid supercapacitors, also known as asymmetric supercapacitors, are a promising class of energy storage devices that combine the advantages of both EDLCs and pseudocapacitors. They typically consist of two different electrode materials with distinct charge storage mechanisms. One electrode utilizes the electrical double-layer capacitance to achieve rapid charge and discharge rates, providing high power density. Meanwhile, the other electrode employs faradaic redox reactions, offering higher energy storage capacity. This combination allows hybrid supercapacitors to balance high power delivery and enhanced energy storage capabilities [14]. By leveraging the strengths of both components, hybrid supercapacitors hold significant potential for various applications, including electric vehicles, renewable energy systems, and portable electronics, where their superior performance and prolonged cycle life can contribute to more efficient and sustainable energy solutions.

1.5.1 Design and Components of Supercapacitors

The basic design of a supercapacitor varies based on its charge storage mechanism. In an Electric Double-Layer Capacitor (EDLC), the core components are two high-surface-area electrodes separated by an ion-permeable separator. Pseudocapacitors also include these components, but they also integrate a specialized material on the electrodes that can undergo redox reactions, boosting their capacitance. Hybrid capacitors combine features of both EDLCs and pseudocapacitors, usually incorporating a combination of materials to achieve enhanced energy and power density.

For a considerable time, conventional supercapacitors fabricated from rigid and bulk materials have served as the foundation of energy storage technology, delivering effective charge and discharge functionalities across diverse applications. However, due to their bulky and rigid design, conventional supercapacitors need help fitting seamlessly into portable and wearable electronic devices.

The bulkiness and rigidity of conventional supercapacitors exhibit challenges in achieving seamless integration into portable systems where compactness and lightweight design are crucial. With the increasing demand for mobile healthcare devices, wearable electronics, and Internet of Things (IoT) devices, the necessity for flexible and lightweight power solutions has risen [15,16]. As a result of this increasing demand, wearable supercapacitors have become a topic of significant interest. The unique characteristics of wearable supercapacitors make them ideal for various applications, including smartwatches, fitness trackers, medical sensors, and other portable healthcare devices. As the world increasingly embraces wearable technology and mobile electronics, the research and development of flexible and wearable supercapacitors remain at the forefront of energy storage innovation, addressing the rising need for lightweight, adaptable, and efficient power sources [17].

The electrolyte, another component of a supercapacitor, which is usually an aqueous or organic solution, facilitates the ion movement between the electrodes during the charge storage process. The separator keeps the electrodes from making electrical contact, while the current collector allows efficient current flow to and from the capacitor. These components form a versatile energy storage system with promising applications in various fields, including portable electronics, renewable energy, and electric vehicles.

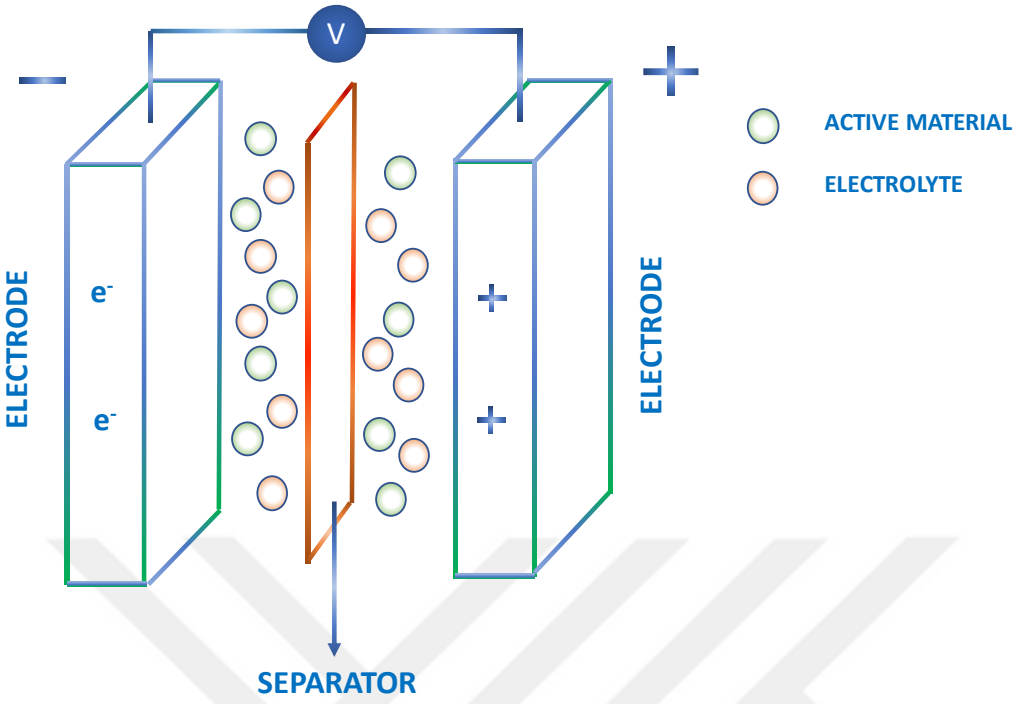

Figure 1-2 A schematic representation of a supercapacitor.

1.5.1.1 Electrode Materials for ECs

The electrodes in supercapacitors are crucial components that significantly impact these energy storage devices' overall performance and effectiveness. Their primary function involves facilitating the movement of ions, enabling the adsorption and desorption processes during charge and discharge cycles. Subsequent sections provide comprehensive details on each common electrode type individually.

1.5.1.1.1 Carbon-based Electrode Materials

EDLC electrodes for supercapacitors have frequently been made of carbon-based materials such as activated carbon, carbon nanotubes (CNTs), and graphene. These materials are preferred in EDLCs because of their large surface area, low production costs, abundance, and stability [5,9,18]. The cyclic stability of the AC-based electrode appeared promising, with 82.8 % of the capacitance remaining after more than

10,000 cycles [19]. On the other hand, highly porous graphene-based electrodes exhibited 7000 cycles, retaining almost 100% capacitance [20]. CNTs-based electrodes were also used in supercapacitor applications displaying high specific capacitance values up to 411 Fg^{-1} [21].

1.5.1.1.2 Polymer-based Electrode Materials

Conducting polymers were first revealed as promising supercapacitor electrode materials in the 1990s [22]. Compared to many other metal oxides, they have better specific capacitance values and can exhibit compelling performances for both negative and positive electrodes. Common examples of conducting-polymer-based electrode materials include poly(3,4-ethylenedioxythiophene), in short, PEDOT [23], polyaniline (PANI) [24], and polypyrrole (PPy) [25].

1.5.1.1.3 Transition Metal-based Electrode Materials

Transition-metal-based materials are frequently chosen as pseudocapacitive electrode materials due to fast redox reactions on the electrode surfaces. Even though they have better energy density values than EDLC-type electrode materials, they suffer from poor cycle life due to irreversible chemical reactions leading to unpleasing structure and performance variations. Several approaches, including surface engineering, nano structuration, and deposition onto carbonaceous materials, have been suggested to improve the performance of SCs [9].

Transition metal oxides, metal nitrides, and metal sulfides are among the materials that have received the most attention as redox pseudocapacitive electrodes [5,18,26,27] At specific potentials, the multiple oxidation states that these metal oxides undergo result in enhanced specific capacitance values. Among metal oxides, RuO_2, MnO_2, Co_3O_4, NiO, and V_2O_5 are frequently researched [18]. Due to its toxicity and high costs, alternatives aside from RuO_2 are examined. Even though RuO_2 has great specific capacitance values after surface engineering and using bimetallic oxides, transition

metal-oxide-based materials reached promising performances [28]. However, Bimetallic sulfides exhibit improved electrochemical activity due to the sulfur atoms' less electronegative character facilitating rapid electron transfers within a more flexible phase structure [4,29]. For supercapacitor applications, a variety of bimetallic-sulfide-based electrodes, including $CuFeS_2$ [30], $CuCo_2S_4$ [31], $MnCo_2S_4$ [32], and $NiCo_2S_4$[33] were utilized, and encouraging results were obtained.

1.5.1.2 Electrolyte

In a supercapacitor, energy density, *E*, is directly proportional to the square of applied potential, V^2, and capacitance, *C*, according to the equation:

$$\mathrm{E} = \frac{1}{2}\mathrm{CV}^2$$

while power density, *P*, can be calculated according to the below equation:

$$P = \frac{\mathrm{V}^2}{4\mathrm{ESR} * \mathrm{m}^2}$$

where ESR stands for the equivalent series resistance and *m* represents the mass of two electrodes. These are two of the key metrics when expressing the actual performance of a supercapacitor. An electrolyte should have a high ionic conductivity to reduce resistance, a wide electrochemical stability window to increase voltage, and close contact with the electrode to create a favorable interface to increase capacity, leading to high energy and power densities [34]. Therefore, while building highly-performing supercapacitors, proper electrolyte selection is essential. The following sections cover each type of electrolyte in detail.

1.5.1.2.1 Aqueous Electrolytes

Aqueous electrolytes are among the most common and widely used types in supercapacitors. Composed of water-based solutions containing dissolved salts like

potassium hydroxide (KOH) or sodium sulfate (Na_2SO_4), they offer several advantages, including cost-effectiveness and ease of preparation. Moreover, these electrolytes exhibit exceptional ionic conductivity, enabling rapid ion movement within the capacitor and facilitating efficient charging and discharging processes [35]. However, their relatively limited voltage window restricts the energy density, making them ideal for low-to-medium-power applications.

1.5.1.2.2 Organic Electrolytes

Organic electrolytes are formulated by blending non-aqueous solvents with suitable electrolyte salts. Commonly employed organic compounds like acetonitrile, propylene carbonate, or ethylene carbonate are combined with lithium salts or other ionic species to create these electrolytes. One distinctive advantage of organic electrolytes is their broader voltage window compared to aqueous electrolytes, contributing to enhanced energy density and capacitance [35,36]. Consequently, they are well-suited for applications requiring elevated power output and prolonged discharge durations. Nevertheless, it is crucial to consider safety concerns since certain organic solvents utilized in these electrolytes can pose flammability and potential toxicity risks.

1.5.1.2.3 Ionic Liquid Electrolytes

Ionic liquids represent a distinct category of electrolytes characterized by exceptional properties that distinguish them from aqueous and organic electrolytes. These electrolytes are essentially room-temperature molten salts consisting of large, asymmetric organic cations paired with small anions [37]. Notably, ionic liquids exhibit remarkable thermal stability, minimal vapor pressure, and excellent electrochemical stability. Due to these characteristics, supercapacitors incorporating ionic liquids demonstrate elevated energy density, superior cycle life, and enhanced safety [38].

Despite these advantages, their adoption has been somewhat constrained due to higher costs and challenging synthesis procedures associated with ionic liquids [39].

1.5.1.2.4 Solid Polymer Electrolytes

As a solid polymer electrolyte, gel polymer electrolytes have gained significant attention due to their ability to combine the characteristics of both liquid and solid electrolytes, making them attractive for various applications. These versatile materials serve as adequate electrolytes and function as separators, offering a promising solution for enhancing the performance and safety of energy storage devices and other electrochemical systems [40]. They encompass a polymer matrix infused with liquid electrolyte, offering improved mechanical stability while sustaining high ionic conductivity. The gel-like architecture effectively hinders electrolyte leakage, rendering them well-suited for flexible and compact supercapacitor configurations. Gel electrolytes also address safety concerns by minimizing the risk of flammability associated with some liquid electrolytes [40].

1.5.1.3 Separators

Separators play a crucial role in supercapacitors by physically and electronically separating the two electrodes while allowing the ionic transport necessary for charge storage. These thin, porous membranes prevent direct contact between the positive and negative electrodes, thereby preventing short circuits and ensuring the safe and efficient operation of the supercapacitor [41]. Additionally, low electrical resistance in separators enables rapid ion movement between the electrodes during charge and discharge, leading to enhanced power performance. Properly selected and designed separators are vital for optimizing supercapacitor performance, energy density, and lifespan across various applications.

1.6 Electrochemical Characterization Methods

1.6.1 Cyclic Voltammetry (CV)

CV is an electrochemical technique to examine the redox behavior of the cell under study. By applying a potential to the working electrode, a flowing current in the system is obtained as a function of the applied potential. From this experiment, a current versus potential plot, which is called a 'voltammogram,' is achieved. These voltammograms give much valuable information about the system under study, such as reversibility, reaction mechanisms on the electrode surface, oxidation and reduction potentials, etc. There are some distinct voltammogram shapes for energy storage applications to characterize if the system under the study shows a supercapacitor-type or battery-type behavior.

Generally, because EDLCs are double-layer in nature, they store the charges non-faradaically, meaning no redox peaks are observed at voltammograms, resulting in rectangular voltammograms (Figure 1-3a). Since pseudocapacitive electrodes are faradaic in nature and the charge is stored electrochemically, redox peaks are observed in voltammograms as in Figure 1-3(b-c). But, when the extent of faradaic charge storage surpasses that of electrostatic charge storage (resembling battery-like behavior), redox peaks become more pronounced in the cyclic voltammetry (CV) profiles for both pseudocapacitors and hybrid supercapacitors as in Figure 1-3c.

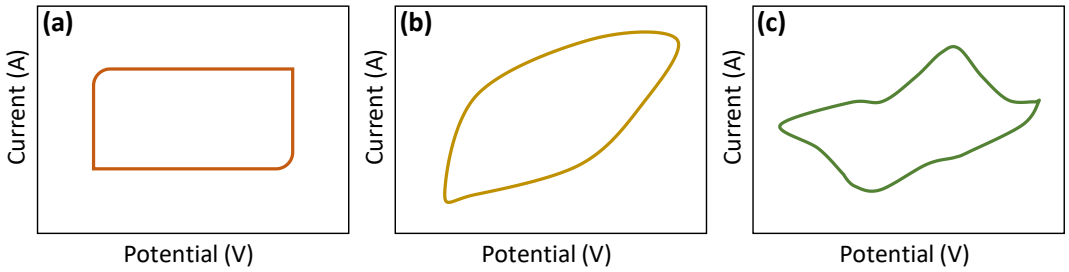

Figure 1-3 A schematic illustration of the characteristic voltammograms of (a) EDLC-type, (b) Pseudocapacitive/hybrid-type, (c) pseudocapacitive/hybrid-type (battery-like) supercapacitors based on their charge storage mechanisms.

1.6.2 Galvanostatic Charge-Discharge Curves (GCD)

Galvanostatic charge-discharge is another technique to measure the material's capacitance under study. In the GCD method, the working electrode is typically charged to a predetermined voltage to measure the capacitance, and the discharge process is then observed. GCD technique can be applied to both three-electrode and two-electrode cell configurations, allowing the determination of specific energy, power density, and cycle stability of the cell.

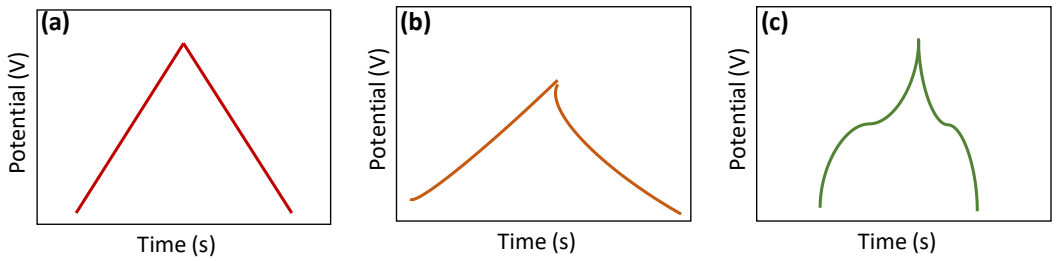

Figure 1-4 A schematic illustration of the characteristic GCD curves of (a) EDLC-type, (b) Pseudocapacitive/hybrid-type, (c) battery-like pseudocapacitive/hybrid-type supercapacitors based on their charge storage mechanisms.

Pseudocapacitive materials deviate from linearity in charge-discharge processes due to the redox reactions as in Figure 1-4(b-c), while EDLC materials charge and discharge linearly (Figure 1-4a). Because of this behavior, EDLC and pseudocapacitive materials have unique equations to calculate their capacitance. For EDLC-type materials, calculations can be done accordingly [18]:

$$C = \frac{I}{dV/dt}$$

where C represents the capacitance, I is the applied current, and dV/dt is the slope of the discharging curve. In pseudocapacitive materials, the equation slightly evolves to the below equation:

$$C = \frac{(\Delta t)(I)}{\Delta V}$$

where Δt shows total discharge time, I is the applied current, and ΔV is the potential difference in the discharging process. To obtain specific capacitance C_{sp}, capacitance value C can be divided by the mass of active materials as in the CV technique.

Both CV and GCD curves can also be used to calculate energy and power density of the fabricated cells and they give valuable information about the real-life applications and stability of the prepared design. Energy and power densities can be calculated accordingly:

$$E = \frac{1C_{SP}\Delta V^2}{2}\ Wh.kg^{-1}$$

$$P = \frac{\Delta V^2}{4mR_{ESR}}\ W.kg^{-1}$$

where C_{sp} is the specific capacitance, ΔV is the potential window, m mass of the active material, and R_{ESR} equivalent series resistance (ESR) within the cell resulting from the resistance of the electrolyte and components from the cell design.

1.6.3 Electrochemical Impedance Spectroscopy (EIS)

The resistance to the flow of an alternating current (AC) is quantified using electrochemical impedance spectroscopy. Unlike other procedures conducted through direct current (DC) techniques, the EIS technique is frequently classified as an AC approach because it typically uses a sinusoidal waveform. In this technique, a sinusoidal potential or a sinusoidal current is swept to measure the impedance of the system as a function of frequency [42]. Because all electrochemical processes on the electrode occur at specific frequencies, one can investigate how diffusion and charge transfers happen in the system, artifacts in device components, equivalent series resistance (ESR) of the cell, interfacial impedance, and the existence of faradaic reactions. For impedance data to make sense, the Bode plot and Nyquist plot exist, and the Nyquist plot is commonly used when reporting data [42,43]. Nyquist plots consist of a y-axis representing imaginary impedance value and an x-axis representing real impedance value. These axes should be in a one-to-one ratio, forming a square plot from high-frequency to low-frequency regime, as shown in Figure 1-5.

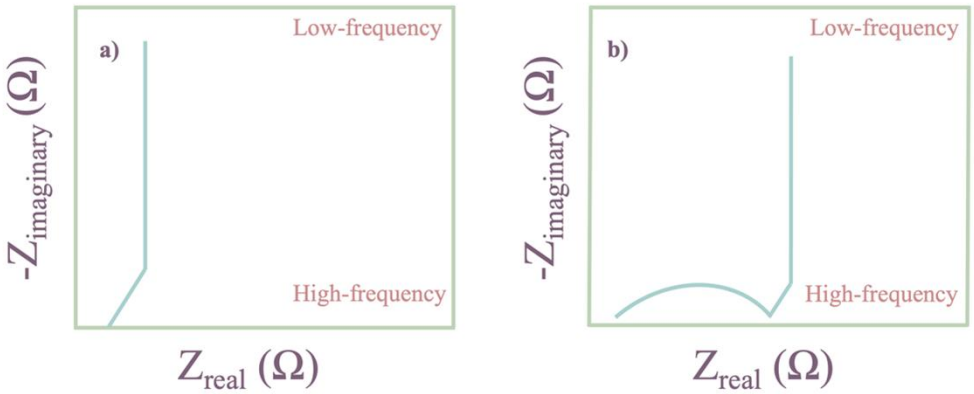

Figure 1-5 A schematic illustration of a Nyquist Plot of (a) double layer and (b) pseudocapacitive type material.

Characteristic semi-circles give the idea of the existence of contributions of charge transfer processes. That's why in double-layer type capacitors, because charge storage occurs electrostatically, semi-circles will not be observed. Instead, a 45° line is observed, followed by a line nearly parallel to the imaginary impedance axes in low-frequency regimes. In contrast to EDLCs, pseudocapacitive materials create semi-circles intersecting real impedance axes in high-frequency regimes, interpreting the real charge transfer resistance value of the electrochemical cell to make sure whether the semi-circle formed because of faradaic reactions, impedance spectra of the cell is recorded under various potentials to see if the shifts are observed for charge transfer resistances.

CHAPTER 2

EXPERIMENTAL

2.1 Materials

All materials were used without further purification. Iron (II) chloride tetrahydrate ($FeCl_2.4H_2O$, ≥ 99.0, Sigma-Aldrich), manganese (II) chloride tetrahydrate ($MnCl_2.4H_2O$, ≥ 99.0, Sigma-Aldrich), thioacetamide (C_2H_5NS, Supelco, GR for analysis ACS, Reag. Ph Eur) were purchased from Sigma-Aldrich. Deionized water (DIW) with a resistivity of 18.2 MΩ (PURELAB Option-Q, ELGA) was used for the solution preparation. Commercial carbon cloth (W0S 1009) was purchased from China for electrode preparation.

2.2 Preparation of Oxygen-Plasma-Modified Carbon Cloth

Carbon cloth (CC) was cut into pieces with sizes of 2 cm x 1 cm as a substrate and sonicated for 15 minutes with acetone, ethanol, and DIW, respectively. After drying, CC was treated in the atmosphere of oxygen plasma for 15 min to obtain a hydrophilic surface using the FEMTO Science Cute Plasma System.

2.3 Fabrication of Flexible Electrodes on Carbon Cloth

$FeCl_2.4H_2O$ (5 mmol), $MnCl_2.4H_2O$ (5 mmol), and thioacetamide (10 mmol) were added to 30.0 mL isopropanol and 10.0 mL DIW and stirred at ambient temperature. After complete dissolution, as-prepared CC was added to the reaction mixture and transferred into a 100 mL Teflon-lined stainless-steel autoclave to be kept at 120 °C

for 48 h. After the reaction, the cloth was washed with DIW to remove residues, while the precipitate was centrifuged with ethanol and DIW following the collection for further characterization processes. The resulting electrode is named MFS-CC. The same procedure was applied to obtain the growth of manganese sulfide on CC without using an iron precursor called MS-CC.

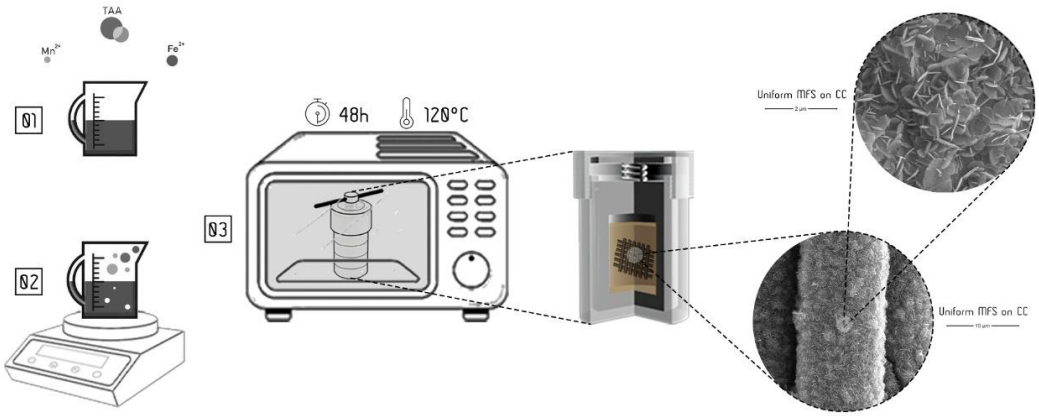

Figure 2-1 A schematic illustration of the experimental process.

2.4 Materials Characterizations

Scanning Electron Microscopy (SEM) images and EDX mappings were obtained using a QUANTA 400F Field Emission microscope. Transmission Electron Microscopy (TEM) images were captured on a Jeol JEM 2100F electron microscope operating at an acceleration voltage of 300 kV. X-ray diffraction analysis was conducted using a Rigaku D/Max-2000 diffractometer with Cu Kα radiation, scanning at a rate of 1°/min. Raman spectra were acquired with a Renishaw inVia Raman spectrometer, using a 532 nm laser. For X-ray photoelectron spectroscopy (XPS), a PHOIBOS instrument equipped with a hemispherical analyzer (HSA3500) and a dual aluminum anode (Al 1486.65 eV) X-ray source was utilized.

2.5 Electrochemical Characterizations

All electrochemical measurements were performed using a Biologic VMP3 Potentiostat/Galvanostat in three and two-electrode setups. Working electrodes consisted of MFS-CC, a saturated calomel electrode served as the reference electrode, and a platinum sheet acted as the counter electrode. The electrolyte used for all measurements was a 1 M potassium hydroxide solution.

To create the flexible device and conduct two-electrode measurements, a mixture of carbon black and activated carbon, along with N-methyl-2-pyrrolidone (NMP) and polyvinylidene fluoride (PVDF) in an 80:15:5 ratio, was sonicated for 45 minutes to prepare the positive electrode. Using a brush, the resulting slurry was employed onto the CC surface (1 x 2 cm2) in a thin coat and left overnight at 100°C in a vacuum oven named AC-CC. The amount of active material loaded was determined by measuring the weight difference before and after slurry coating. Subsequently, the as-prepared MFS-CC served as the negative electrode, while AC-CC acted as the positive electrode.

A cellulose-based gel electrolyte was prepared by heating hydroxyethyl-cellulose with 60 mL of deionized water until a clear solution formed. After the solution turned into a gel, 6 g of 10 M KOH was gradually added and allowed to cool to room temperature. Then, 0.2 g of glycerol was added and mixed in. A disposable non-woven cloth was coated with a thin layer of this gel electrolyte used as a separator. The electrodes were sealed using PVC lamination, and untreated hydrophobic CC was employed for the contacts. The resulting device was given the designation MFS-CC//AC-CC.

CHAPTER 3

RESULTS AND DISCUSSION

3.1 Structural and Morphological Characterizations of MFS-CC

MFS nanoplatelets were directly grown on the fibers of the CC by hydrothermal method (more details in the experimental section). Morphology and the fabricated electrodes' structure were investigated using SEM. Figure 3-1(a-c) shows SEM images in different magnifications, revealing that the carbon cloth's surface was changed to become hydrophilic after activation, resulting in a more homogeneous coating on the cloth’s fibers.

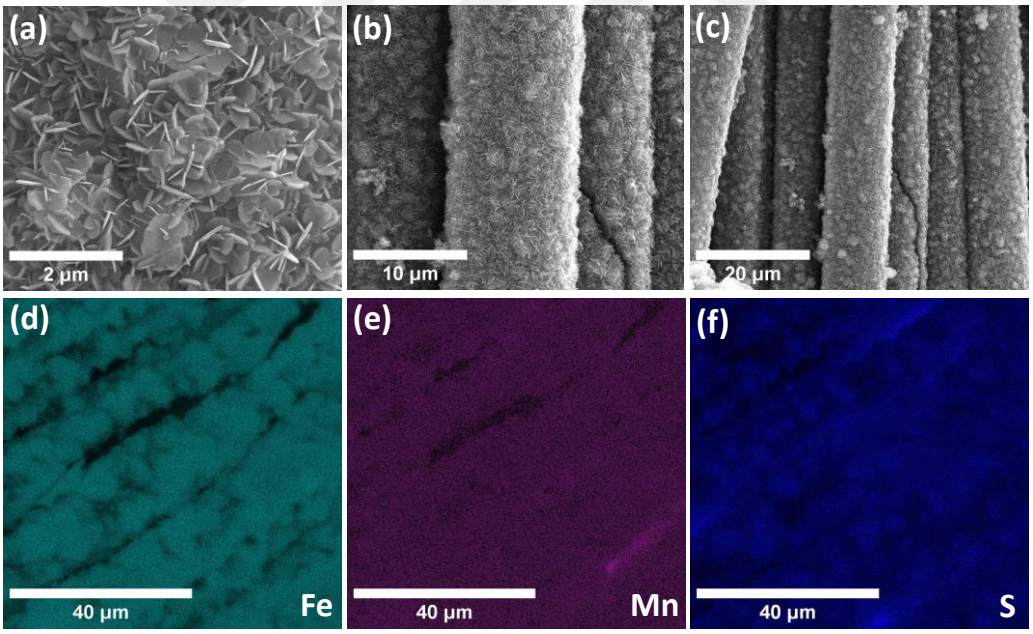

Figure 3-1 (a-c) SEM images of the synthesized material on CC from high magnification to low magnification. Elemental mapping of the synthesized material on CC (d) Fe, (e) Mn, (f) S.

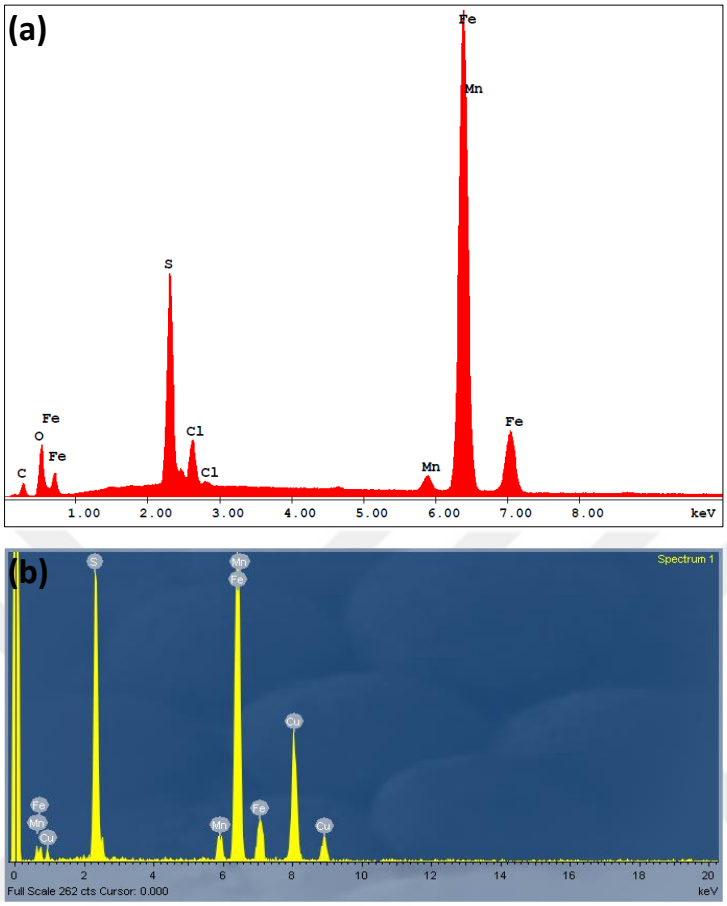

Figure 3-2 (a) EDX pattern of the synthesized material, (b) full survey spectrum of the synthesized material.

The synthesized material has a uniform, porous, nanoplatelet-like morphology throughout the 3D fiber network, which may facilitate ionic transport through electrochemical reactions and provide more electro-active sites for energy storage applications [44]. Elemental mapping was conducted to further evaluate the chemical composition through the fibers of the carbon cloth, indicating the presence of Fe, Mn, and S (Figure 3-1(d-e-f)). Also, EDX analysis was used to confirm that prepared electrodes consist of Mn, Fe, and S elements in the structure (Figure 3-2a).

A TEM study was carried out to examine the MFS structure further. The nanoplatelet structure with hexagonal sharp edges was evident in alignment with the SEM images (Figure 3-3(a-c)). Iron, sulfur, and manganese elements in the matrix are further demonstrated by the full spectrum shown in Figure 3-2b.

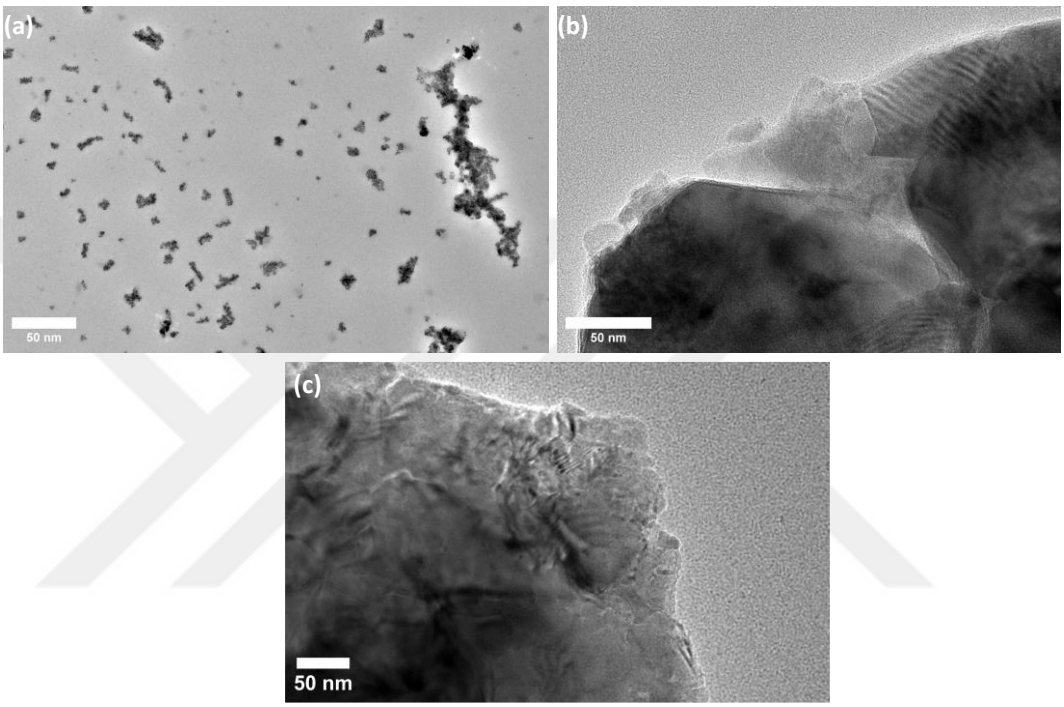

Figure 3-3 (a-c) TEM images of the synthesized material in different magnifications.

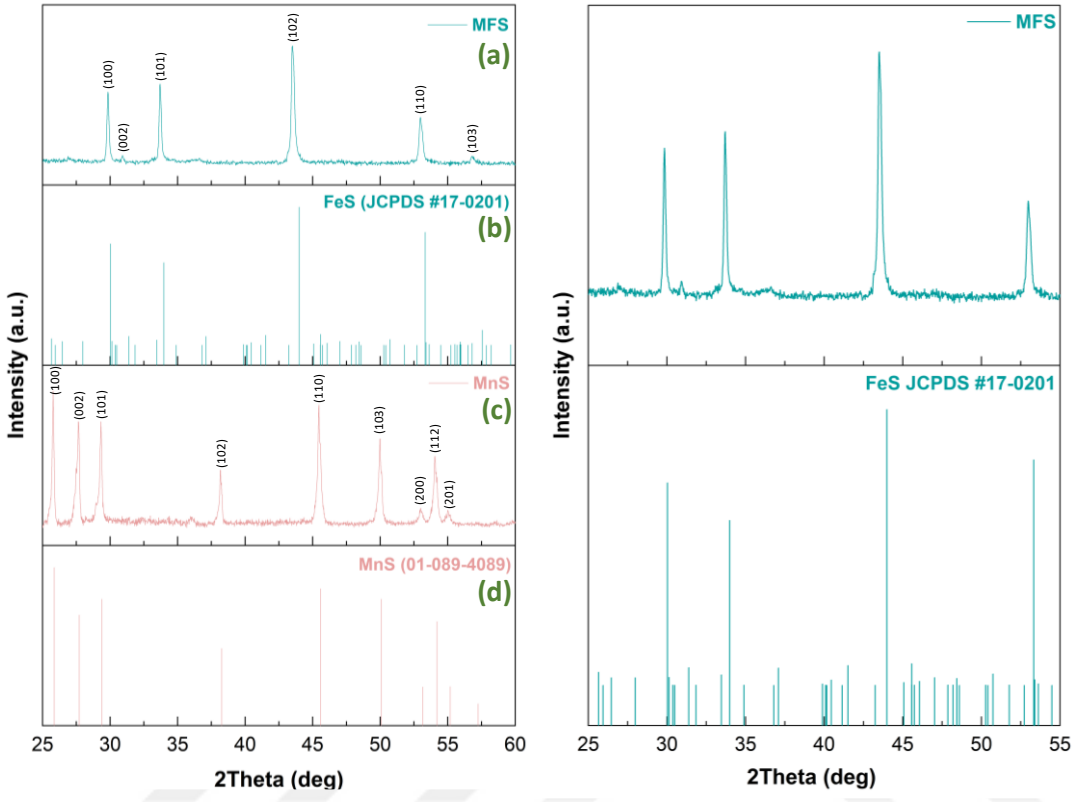

Figure 3-4 XRD pattern of the (a) MFS powder, (b) hexagonal pyrrhotite FeS structure, (c) MnS powder, and (d) hexagonal wurtzite MnS structure. Enlarged view of MFS powder pattern (top) and the hexagonal pyrrhotite FeS pattern (bottom) on the right-hand side.

Figure 3-4 shows the X-ray diffraction (XRD) patterns for both MFS and MnS powders. The distinct and well-defined diffraction peaks prominently indicate the crystalline nature of the as-synthesized materials. The observed XRD peaks correspond to the diffraction pattern attributed to the hexagonal $Fe_{1-x}S$ structure and hexagonal MnS based on JCPDS no. 17-0201 and 01-089-4090. Notably, the XRD patterns of the samples exhibit excellent agreement with the hexagonal pyrrhotite $Fe_{1-x}S$ structure, with no evidence of a discernible impurity phase. Significantly, the XRD peak positions in the MFS nanoplatelets show a minor shift towards lower degrees. This shift serves as evidence of the effective incorporation of Mn^{2+} ions into

the pyrrhotite host matrix. This incorporation arises from the larger atomic radius of Mn in comparison to Fe, facilitating the doping of Mn atoms into the FeS lattice and consequently leading to expanded lattice parameters. Consistent with the Bragg equation, the spacing between crystal planes is inversely related to the diffraction angle, thereby contributing to the reduction in the diffraction angle.

Importantly, the absence of MnS peaks within the XRD pattern of MFS strongly implies the proposition that Mn atoms are successfully doped within the FeS lattice rather than forming a distinct FeS/MnS compound [45]. Synthesizing stable nanoscale iron sulfides presents inherent challenges, predominantly owing to the strong tendency of ferric ions to associate with oxygen, potentially yielding iron oxides during the synthetic process [46]. Adding the manganese precursor during the hydrothermal reaction is believed to stabilize the FeS structure. This, in turn, helps Mn atoms to be effectively doped and stabilize the pyrrhotite structure even at lower temperatures.

The surface chemistry of both MFS and MnS powders was examined by XPS analysis, proving the existence of Fe, Mn, and S elements in full survey-scan spectra as in Figure 3-5a. The presence of O 1s peaks on the spectrum suggests that the sample has undergone oxidation following exposure to the open-air environment.

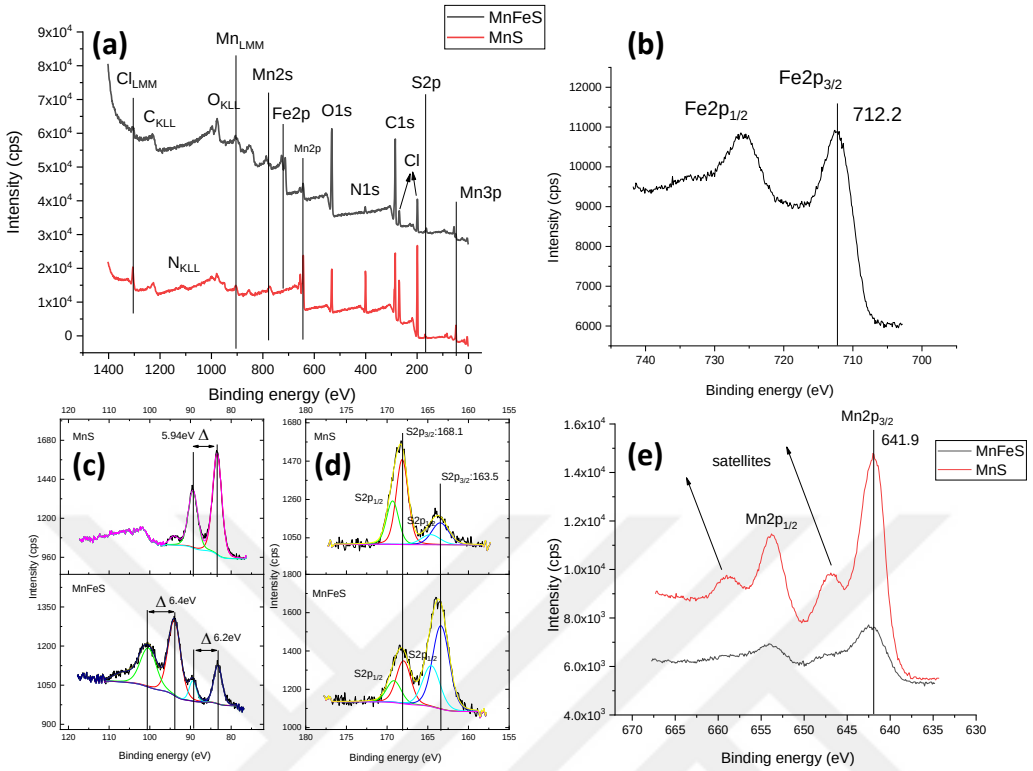

Figure 3-5 The XPS spectra of (a) survey, (b) Fe 2p, (c) Mn 3s, (d) S 2p, (e) Mn 2p.

For the Fe 2p spectrum, Figure 3-5b indicates the presence of Fe^{3+} with the two located peaks analogous to $Fe2p_{3/2}$ and $Fe2p_{1/2}$, respectively [47]. The Mn 2p spectrum for both MnS and MFS cases displays two satellite peaks, Mn $2p_{3/2}$ and $Mn_{2p1/2}$, stating the presence of manganese ions in the +2 valence state (Figure 3-5e). Fig. 3-5d exhibits the XPS spectra of S 2p for both MnS and MFS samples. Two major peaks were observed corresponding to sulfite at 163.5 eV and polysulfide S_n^{2-} (n<2) and/or disulfide S^{-2} at 168.1 eV. Also, the peak at 163.5 eV can be ascribed to the bond between iron and sulfur atoms [48]. Due to the overlapping nature of various oxidation states in manganese samples, the individual Mn 3s spectrum was also studied (Fig. 3-5c). The average oxidation state of both synthesized materials was determined by measuring peak splitting energy separation, ΔE, which came out as

5.94 eV for MnS and 6.2 eV for MFS, implying that the +2 oxidation state of Mn present in both cases, which is consistent with previous reports [49,50].

3.2 Electrochemical Characterizations

The electrochemical performance of the as-prepared electrodes was evaluated in a three-electrode cell configuration using 1 M KOH electrolyte at room temperature by performing CV, GCD, and EIS techniques. The CV, GCD, and EIS profiles of the MFS electrode are shown in Figure 3-6.

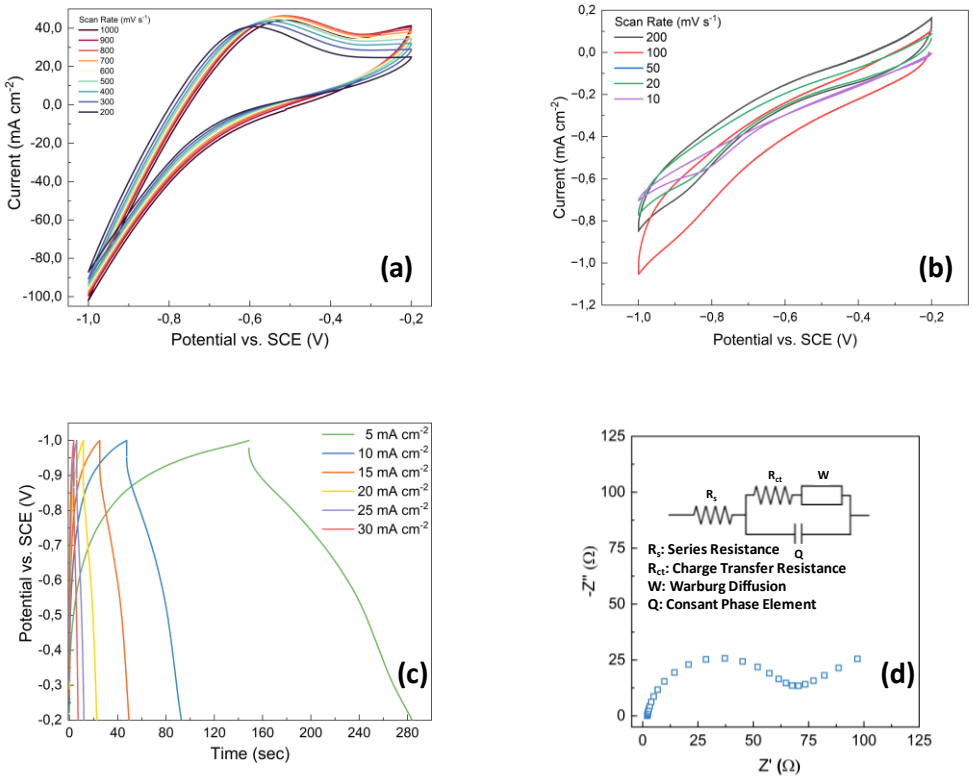

Figure 3-6 (a) CV profile of MFS-CC, (b) CV profile of MS-CC, (c) GCD curve of MFS-CC, (d) EIS data of MFS-CC with the EIS model inset.

Figure 3-6(a-b) shows the MFS-CC electrode and MS-CC CV curves at various sweep rates in the potential window of -1.2 V to -0.2 V. Figure 3-6a clearly exhibits

a higher CV integrated area than the CV curves of MS-CC (Figure 3-6b), indicating better electrochemical activity. The storage mechanism of FeS in a 1 M KOH solution is likely attributed to the reversible transformation between FeS and Fe_3O_4. This can be proposed in the following mechanism [51]:

$$3FeS + 8OH^- \rightleftarrows Fe_3O_4 + 3S^{2-} + 2e^-$$

$$Fe + 2OH^- \rightarrow Fe(OH)_2 + 2e^-$$

Oxidation-reduction peaks signify a substantial contribution of Faradaic mechanisms to the overall capacitance. The nearly symmetrical nature of the peaks observed in the created electrodes demonstrates a reversible "pseudocapacitive" redox behavior. When scanned at a rate of 10 mVs^{-1}, the fabricated electrode displays a maximum specific capacitance of 206 F/g. This achievement surpasses the specific capacity of 189 F/g demonstrated by the $FeMnO_3$/rGO composite electrode despite the noted enhanced electrochemical performance associated with rGO composites [52]. The observed capacitance value is attributed to the synergistic effects arising from the electroactivity of sulfur combined with the 3D network structure of the fibers. Table 3.1 provides comparative data of previous studies based on their respective specific capacity values.

Table 3. 1 Various transition-metal-sulfide-based materials and their corresponding specific capacitance values.

Electrode Material	Scan Rate/Current Density	Specific Capacitance	Reference
MFS-CC	10 mV s^{-1}	206 F/g	Current work
$FeMnO_3$ Hollow Sphere	10 mV s^{-1}	90 F/g	[52]
$FeMnO_3$ nanobelts	10 mV s^{-1}	160 F/g	[53]
$MnFe_2O_4$ nanosheets	10 mA cm^{-2}	234.8 mC cm^{-2}	[54]
FeS-based	5 mV s^{-1}	281 F/g	[55]
Hollow urchin γ-MnS	1 A/g	198 F/g	[56]
Mn-Fe-S	2 mA cm^{-2}	795.7 mF cm^{-2}	[57]

Moreover, the GCD curves illustrate typical pseudocapacitive behavior (Figure 3-6c). The presence of plateaus in the GCD curves indicates a redox reaction consistent with the findings from the CV curves. The MFS electrode exhibits favorable Coulombic efficiency and outstanding reversibility, as evident from the nearly symmetrical charge-discharge curve profiles.

The electrochemical impedance spectroscopy of MFS-CC is depicted in Figure 3-6d, revealing a low equivalent series resistance (ESR) characterized by a concise semicircular shape at high frequency. A smaller semicircle diameter corresponds to a lower charge transfer resistance within the electrochemical system. These characteristics can be ascribed to several underlying factors. Firstly, the ultra-porous and nano-platelet architecture of MFS facilitates a wealth of electro-active sites, thereby enhancing the occurrence of redox reactions [58]. Secondly, the direct growth between the fibers and MFS results in the formation of numerous three-dimensional networks, facilitating efficient electron transport during the charge transfer process [59].

A complete cell configuration was devised for flexible device applications, incorporating MFS-CC and AC-CC electrodes as the negative and positive terminals, respectively, along with a cellulose-based gel electrolyte. The assembly of this device is depicted in Figure 3-7f, and comprehensive details can be found in the experimental section.

Figure 3-7a displays cyclic voltammetry (CV) curves obtained at various scan speeds ranging from 0.0 V to 1.4 V. The presence of redox peaks indicates the pseudocapacitive nature of the constructed device, while the quasi-rectangular shapes of the curves signify near-optimal supercapacitor performance. Notably, the CV curves maintain similar forms across varying scan rates without distortion, indicating the device's outstanding charge/discharge capabilities.

The electrochemical performance of the fabricated device was thoroughly assessed through galvanostatic charge-discharge (GCD) tests conducted over a wide range of current densities, varying from 1 to 5 mA cm^{-2}. Notably, all the GCD curves

exhibited symmetrical and linear behavior, indicating the device's excellent reversibility and capacitive characteristics (Figure 3-7c).

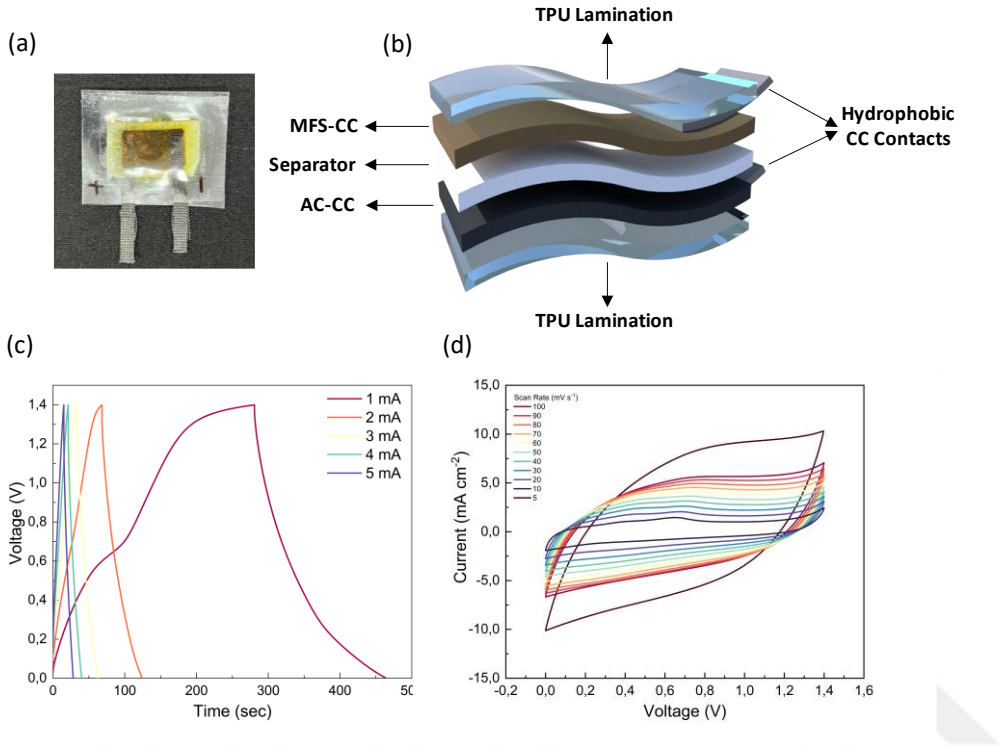

Figure 3-7 (a) an actual photograph of the device design, (b) schematic representation of the wearable and flexible device, (c) GCD curves at different current densities, and (d) CV profile at different scan rates.

To further demonstrate its capability and durability, the electrochemical stability of the device was evaluated, demonstrating an impressive total of 11000 cycles. As illustrated in Figure 3-7d, the results exhibit the enhanced performance of the manufactured electrode, showing no capacitive retention throughout the charge/discharge operations and no observable structural changes even after such an extensive cycling process. The remarkable stability observed in MFS-CC is believed to arise from an electro-activation process involving the active materials. This process leads to prolonged operation over numerous cycles, enabling deeper

penetration and activation of the bulk materials in conjunction with the gel electrolyte [60,61].

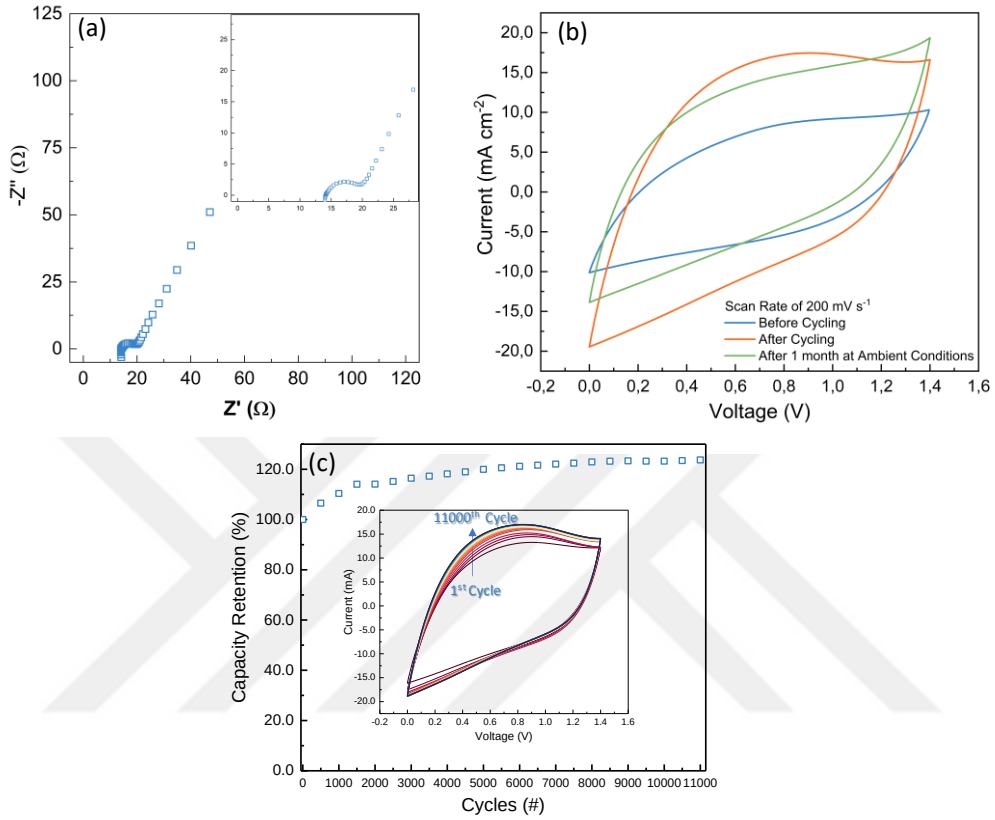

Figure 3-8 (a) EIS data, (b) stability test at 200 mVs^{-1}, and (c) CV profile for 11000 cycles.

Their integrated system was further examined in series and parallel configurations to assess the practical applicability of the fabricated supercapacitors. The physical arrangement of the actual device, along with a self-powered flexible device and a light-emitting diode (LED) embedded in a hoodie for practical use, is depicted in Figure 3-9(c-f).

Cyclic voltammetry (CV) and galvanostatic charge-discharge (GCD) profiles of the single-fiber device, two and three-fiber devices connected in series are shown in

Figure 3-9a. Comparatively, the series connection of two and three supercapacitors resulted in a broader potential window of 3 V and 4 V, respectively, compared to a single device operating at 1 V. Similarly, when two or three devices were linked in series, there was an observable increase in the output current in CV curves and an extended discharge time in GCD curves, compared to a single device operating at the same constant current value of 10 mA cm^{-2} (Figure 3-9(a-d)).

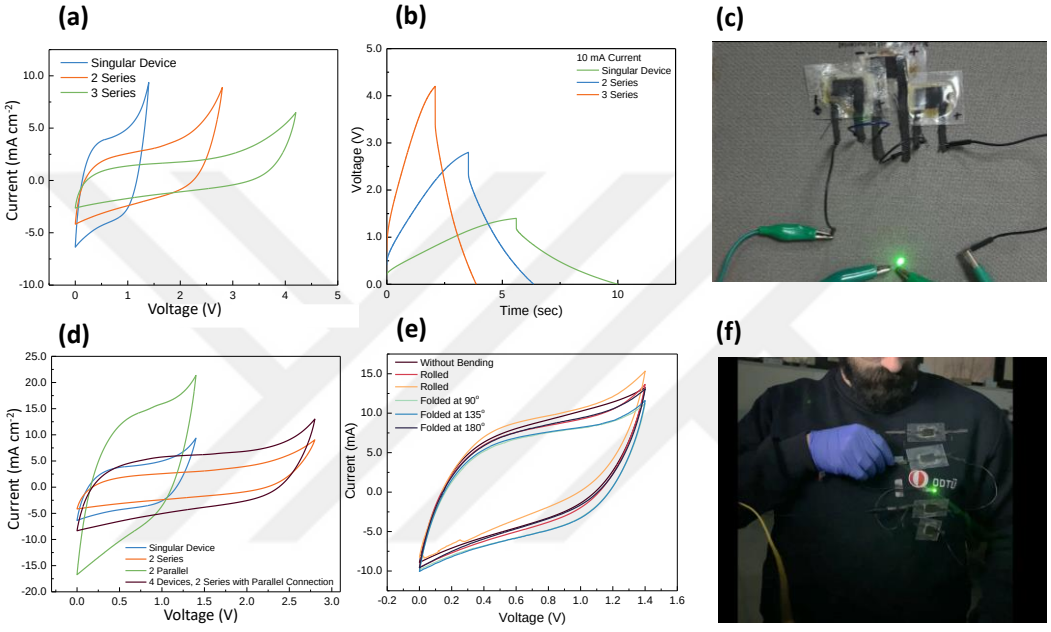

Figure 3-9 (a,d) CV scans of the singular device, series and parallel configurations, (b) GCD profiles of the singular device and series configurations, (c) an actual photograph of self-powered MFS-CC//AC-CC flexible device, (e) CV profile of the as-fabricated device under various bending scenarios, and (f) the image of green LED embedded in a hoodie with lights on.

The integrated fiber supercapacitors also demonstrated outstanding pseudocapacitive characteristics, irrespective of whether they were arranged in series or parallel configurations. This further substantiates their potential to be interconnected in different setups, serving as power sources for a diverse range of flexible electronic devices operating with alternative voltage sources (Fig. 3-9d). The CV profile of the as-fabricated device, acquired at a scan rate of 200 mVs^{-1}, is illustrated in Figure 3-

9e, showcasing its response under various bending conditions. Notably, all CV curves, including those obtained from rolled and folded positions, exhibited remarkably similar patterns, indicating the device's exceptional mechanical robustness. This favorable mechanical resilience makes it highly suitable for integrating into flexible and wearable gadgets, owing to its excellent flexibility and bendability. Fig. 3-9f is a shot of the self-powered flexible device and a green light emitting diode (LED) embedding in a hoodie, showcasing its potential for real-world applications.

Based on the aforementioned results, it is of significance to highlight that the use of MFS-CC holds great promise for improving the electrochemical performance of supercapacitors, leading to higher capacitance, greater rate capability, and superior cyclic stability through the direct growth of CC, which facilitates electron transport and establishes a synergistic effect between the material and 3D fiber network ensuring greater area of surface as well as effective contact with the electrolyte without needing nonconductive binders.

CHAPTER 4

CONCLUSIONS AND FUTURE WORKS

4.1 CONCLUSIONS

In conclusion, this study presents significant progress in developing flexible and wearable supercapacitors, offering potential benefits for energy storage solutions. The direct growth of Mn-doped $Fe_{1-x}S$ nanoplatelets on the fibers of carbon cloth through a simple hydrothermal method represents an exciting approach, eliminating the need for organic binders and enhancing the electrochemical performances of the electrodes as well as enabling the synthesis of a stable pyrrhotite framework, even under lower temperatures.

The homogeneous decoration of MFS on CC results in the creation of abundant electroactive sites, promoting efficient ion transport and improving electrochemical properties. The obtained specific capacitance of 206 F g^{-1} and excellent cyclic stability over 11,000 cycles demonstrate the reliability and durability of the as-prepared electrodes, making them promising for practical applications.

Moreover, encapsulating the as-fabricated electrodes ensures their prolonged efficiency for up to three months, indicating long-term usage and stability feasibility. This extended operational capability is essential for real-world applications, as it seamlessly integrates supercapacitors into various electronic gadgets and smart textiles.

The successful construction of a self-powered flexible supercapacitor incorporating the prepared electrodes showcases the potential of this technology in powering wearable devices. The ability to light up green LED arrays embedded in a hoodie emphasizes the real-world flexibility and wearability of this innovative energy storage solution.

The findings of this study have implications for the future of energy storage and wearable electronics. The developed MFS-CC electrodes open up possibilities for more efficient and durable flexible supercapacitors, which could find applications in various fields, including health monitoring devices and interactive smart clothing.

As the world continues to seek sustainable and eco-friendly energy solutions, the advancements presented in this research contribute to the ongoing efforts. By exploring the unique capabilities of supercapacitors, there is potential to reduce dependence on traditional fossil fuels and embrace a more environmentally conscious approach to energy consumption.

In conclusion, the advancements achieved in this study highlight the potential of flexible and wearable supercapacitors as a promising option for energy storage. This technology may improve portable electronic devices, offering increased convenience, efficiency, and sustainability. As research in this field progresses, we can expect further innovations that may positively impact our daily lives and contribute to a cleaner and more connected world.

4.2 FUTURE WORKS

Subsequent Structural and Electrochemical Characterizations: In-depth examination of the XPS and XRD characterizations to ascertain the dopant concentration and facilitate a comparative assessment of atomic percentages through Energy Dispersive X-ray (EDX) analysis. Additionally, the investigation of the stability of the device encompassing more than 11000 cycles and the development of the EIS model.

Electrolyte Optimization: Investigation of novel electrolyte formulations, including ionic liquids or gel-based electrolytes, to enhance the specific capacitance and overall performance of the supercapacitor.

Integration with Other Devices: Investigation of how these flexible supercapacitors can be integrated into other wearable or portable electronic devices, such as health monitoring devices or IoT sensors.

Material Optimization: Investigation of the impact of different Mn doping levels on the properties of MFS nanoplatelets. This can help identify the optimal composition for even better electrochemical performance.

REFERENCES

1. Jost, K., Dion, G. & Gogotsi, Y. Textile energy storage in perspective. *J. Mater. Chem. A* **2**, 10776 (2014).
2. Dubal, D. P., Chodankar, N. R., Kim, D.-H. & Gomez-Romero, P. Towards flexible solid-state supercapacitors for smart and wearable electronics. *Chem. Soc. Rev.* **47**, 2065–2129 (2018).
3. Muralee Gopi, C. V. V., Vinodh, R., Sambasivam, S., Obaidat, I. M. & Kim, H.-J. Recent progress of advanced energy storage materials for flexible and wearable supercapacitor: From design and development to applications. *Journal of Energy Storage* **27**, 101035 (2020).
4. Gao, Y. & Zhao, L. Review on recent advances in nanostructured transition-metal-sulfide-based electrode materials for cathode materials of asymmetric supercapacitors. *Chemical Engineering Journal* **430**, 132745 (2022).
5. Lu, X., Li, G. & Tong, Y. A review of negative electrode materials for electrochemical supercapacitors. *Sci. China Technol. Sci.* **58**, 1799–1808 (2015).
6. Simon, P. & Gogotsi, Y. Perspectives for electrochemical capacitors and related devices. *Nat. Mater.* **19**, 1151–1163 (2020).
7. Becker, H. J. & Ferry, V. Low voltage electrolytic capacitor.
8. Liu, R. *et al.* Fundamentals, advances and challenges of transition metal compounds-based supercapacitors. *Chemical Engineering Journal* **412**, 128611 (2021).

9. Simon, P. & Gogotsi, Y. Materials for electrochemical capacitors. *Nature Mater* **7**, 845–854 (2008).

10. Chodankar, N. R. *et al.* True Meaning of Pseudocapacitors and Their Performance Metrics: Asymmetric versus Hybrid Supercapacitors. *Small* **16**, 2002806 (2020).

11. Mastragostino, M., Soavi, F. & Arbizzani, C. Electrochemical Supercapacitors. in *Advances in Lithium-Ion Batteries* (eds. Van Schalkwijk, W. A. & Scrosati, B.) 481–505 (Springer US, 2002). doi:10.1007/0-306-47508-1_17.

12. Bhojane, P. Recent advances and fundamentals of Pseudocapacitors: Materials, mechanism, and its understanding. *Journal of Energy Storage* **45**, 103654 (2022).

13. Conway, B. E. Transition from "Supercapacitor" to "Battery" Behavior in Electrochemical Energy Storage. *J. Electrochem. Soc.* **138**, 1539–1548 (1991).

14. Sun, J., Luo, B. & Li, H. A Review on the Conventional Capacitors, Supercapacitors, and Emerging Hybrid Ion Capacitors: Past, Present, and Future. *Adv Energy and Sustain Res* **3**, 2100191 (2022).

15. Zhan, Y., Mei, Y. & Zheng, L. Materials capability and device performance in flexible electronics for the Internet of Things. *J. Mater. Chem. C* **2**, 1220–1232 (2014).

16. Delbari, S. A. *et al.* Transition metal oxide-based electrode materials for flexible supercapacitors: A review. *Journal of Alloys and Compounds* **857**, 158281 (2021).

17. Benzigar, M. R., Dasireddy, V. D. B. C., Guan, X., Wu, T. & Liu, G. Advances on Emerging Materials for Flexible Supercapacitors: Current Trends and Beyond. *Adv. Funct. Mater.* **30**, 2002993 (2020).

18. Kim, B. K., Sy, S., Yu, A. & Zhang, J. Electrochemical Supercapacitors for Energy Storage and Conversion. in *Handbook of Clean Energy Systems* (ed. Yan, J.) 1–25 (John Wiley & Sons, Ltd, 2015). doi:10.1002/9781118991978.hces112.

19. Maher, M., Hassan, S., Shoueir, K., Yousif, B. & Abo-Elsoud, M. E. A. Activated carbon electrode with promising specific capacitance based on potassium bromide redox additive electrolyte for supercapacitor application. *Journal of Materials Research and Technology* **11**, 1232–1244 (2021).

20. Yang, H. *et al.* Graphene supercapacitor with both high power and energy density. *Nanotechnology* **28**, 445401 (2017).

21. Aval, L. F., Ghoranneviss, M. & Pour, G. B. High-performance supercapacitors based on the carbon nanotubes, graphene and graphite nanoparticles electrodes. *Heliyon* **4**, e00862 (2018).

22. Snook, G. A., Kao, P. & Best, A. S. Conducting-polymer-based supercapacitor devices and electrodes. *Journal of Power Sources* **196**, 1–12 (2011).

23. Lota, K., Khomenko, V. & Frackowiak, E. Capacitance properties of poly(3,4-ethylenedioxythiophene)/carbon nanotubes composites. *Journal of Physics and Chemistry of Solids* **65**, 295–301 (2004).

24. Klimont, A. A. *et al.* Polyaniline-Containing composites based on highly porous carbon cloth for flexible supercapacitor electrodes. *J. Synch. Investig.* **11**, 940–947 (2017).

25. Clemente, A. Solid-state, polymer-based, redox capacitors. *Solid State Ionics* **85**, 273–277 (1996).

26. Balaji, T. E., Tanaya Das, H. & Maiyalagan, T. Recent Trends in Bimetallic Oxides and Their Composites as Electrode Materials for Supercapacitor Applications. *ChemElectroChem* **8**, 1723–1746 (2021).

27. Fleischmann, S. *et al.* Pseudocapacitance: From Fundamental Understanding to High Power Energy Storage Materials. *Chem. Rev.* **120**, 6738–6782 (2020).

28. Liu, C. *et al.* Toward Superior Capacitive Energy Storage: Recent Advances in Pore Engineering for Dense Electrodes. *Adv. Mater.* **30**, 1705713 (2018).

29. Li, R., Wang, S., Huang, Z., Lu, F. & He, T. NiCo2S4@Co(OH)2 core-shell nanotube arrays in situ grown on Ni foam for high performances asymmetric supercapacitors. *Journal of Power Sources* **312**, 156–164 (2016).

30. Rupa Ranjani, P., Anjana, P. M. & Rakhi, R. B. Solvothermal synthesis of CuFeS2 nanoflakes as a promising electrode material for supercapacitors. *Journal of Energy Storage* **33**, 102063 (2021).

31. Moosavifard, S. E., Fani, S. & Rahmanian, M. Hierarchical $CuCo_2S_4$ hollow nanoneedle arrays as novel binder-free electrodes for high-performance asymmetric supercapacitors. *Chem. Commun.* **52**, 4517–4520 (2016).

32. Elshahawy, A. M. *et al.* Controllable $MnCo_2S_4$ nanostructures for high performance hybrid supercapacitors. *J. Mater. Chem. A* **5**, 7494–7506 (2017).

33. Chen, H. *et al.* Highly conductive NiCo2S4 urchin-like nanostructures for high-rate pseudocapacitors. *Nanoscale* **5**, 8879 (2013).

34. Virya, A. & Lian, K. A review of neutral pH polymer electrolytes for electrochemical capacitors: Transitioning from liquid to solid devices. *Materials Reports: Energy* **1**, 100005 (2021).

35. Zhao, C. & Zheng, W. A Review for Aqueous Electrochemical Supercapacitors. *Front. Energy Res.* **3**, (2015).

36. Bhat, T. S., Patil, P. S. & Rakhi, R. B. Recent trends in electrolytes for supercapacitors. *Journal of Energy Storage* **50**, 104222 (2022).

37. Zhong, C. *et al.* A review of electrolyte materials and compositions for electrochemical supercapacitors. *Chem. Soc. Rev.* **44**, 7484–7539 (2015).

38. Armand, M., Endres, F., MacFarlane, D. R., Ohno, H. & Scrosati, B. Ionic-liquid materials for the electrochemical challenges of the future. *Nature Mater* **8**, 621–629 (2009).

39. Zhong, C. *et al.* A review of electrolyte materials and compositions for electrochemical supercapacitors. *Chem. Soc. Rev.* **44**, 7484–7539 (2015).

40. Cheng, X., Pan, J., Zhao, Y., Liao, M. & Peng, H. Gel Polymer Electrolytes for Electrochemical Energy Storage. *Adv. Energy Mater.* **8**, 1702184 (2018).

41. Ahankari, S., Lasrado, D. & Subramaniam, R. Advances in materials and fabrication of separators in supercapacitors. *Mater. Adv.* **3**, 1472–1496 (2022).

42. Mathis, T. S. *et al.* Energy Storage Data Reporting in Perspective—Guidelines for Interpreting the Performance of Electrochemical Energy Storage Systems. *Adv. Energy Mater.* **9**, 1902007 (2019).

43. Macdonald, D. D. Reflections on the history of electrochemical impedance spectroscopy. *Electrochimica Acta* **51**, 1376–1388 (2006).

44. You, Y. *et al.* Subzero-Temperature Cathode for a Sodium-Ion Battery. *Adv. Mater.* **28**, 7243–7248 (2016).

45. Chen, H. *et al.* Mn-doped FeS with larger lattice spacing as advance anode for sodium ion half/full battery. *Chemical Engineering Journal* **450**, 137960 (2022).

46. Argueta-Figueroa, L. *et al.* Hydrothermal synthesis of pyrrhotite (Fex-1S) nanoplates and their antibacterial, cytotoxic activity study. *Progress in Natural Science: Materials International* **28**, 447–455 (2018).

47. Jiang, F., Peckler, L. T. & Muscat, A. J. Phase Pure Pyrite FeS $_2$ Nanocubes Synthesized Using Oleylamine as Ligand, Solvent, and Reductant. *Crystal Growth & Design* **15**, 3565–3572 (2015).

48. Arabczyk, W., Baumann, T., Müssig, H.-J., Storbeck, F. & Meisel, A. Interaction between sulphur and oxygen on Fe(111). *Vacuum* **41**, 79–81 (1990).

49. Lee, J. H., Sa, Y. J., Kim, T. K., Moon, H. R. & Joo, S. H. A transformative route to nanoporous manganese oxides of controlled oxidation states with identical textural properties. *Journal of Materials Chemistry A* **2**, 10435–10443 (2014).

50. Mohamed, S. G., Attia, S. Y., Barakat, Y. F., Hassan, H. H. & Zoubi, W. Al. Hydrothermal Synthesis of α-MnS Nanoflakes@Nitrogen and Sulfur Co-doped rGO for High-Performance Hybrid Supercapacitor. *ChemistrySelect* **3**, 6061–6072 (2018).

51. Shao, X., Zhu, Z., Zhao, C., Zhao, C. & Qian, X. Hierarchical FeS/RGO/FeS@Fe foil as high-performance negative electrode for asymmetric supercapacitors. *Inorg. Chem. Front.* **5**, 1912–1922 (2018).

52. Li, M. *et al.* Facile synthesis of specific FeMnO3 hollow sphere/graphene composites and their superior electrochemical energy storage performances for supercapacitor. *Journal of Power Sources* **248**, 465–473 (2014).

53. Wei, H., Guo, Y., Gao, C. & Wang, Z. Solvothermal synthesis of FeMnO3 nanobelts with excellent electrochemical performances for lithium-ions batteries and supercapacitors. *Advanced Powder Technology* **32**, 4322–4329 (2021).

54. Fei, M. *et al.* Epitaxial growth of MnFe2O4 nanosheets arrays for supercapacitor. *Electrochimica Acta* **368**, 137586 (2021).

55. Karade, S. S., Dwivedi, P., Majumder, S., Pandit, B. & Sankapal, B. R. First report on a FeS-based 2 V operating flexible solid-state symmetric supercapacitor device. *Sustainable Energy Fuels* **1**, 1366–1375 (2017).

56. Kumar, S. *et al.* In-Situ Growth of Urchin Manganese Sulfide Anchored Three-Dimensional Graphene (γ-MnS@3DG) on Carbon Cloth as a Flexible Asymmetric Supercapacitor. *J. Phys. Chem. Lett.* **12**, 6574–6581 (2021).

57. Shin, J. C. *et al.* Fabrication and Development of Binder-Free Mn–Fe–S Mixed Metal Sulfide Loaded Ni-Foam as Electrode for the Asymmetric Coin Cell Supercapacitor Device. *Nanomaterials* **12**, 3193 (2022).

58. Javed, M. S. *et al.* Flexible full-solid state supercapacitors based on zinc sulfide spheres growing on carbon textile with superior charge storage. *J. Mater. Chem. A* **4**, 667–674 (2016).

59. Shen, L., Che, Q., Li, H. & Zhang, X. Mesoporous NiCo $_2$ O $_4$ Nanowire Arrays Grown on Carbon Textiles as Binder-Free Flexible Electrodes for Energy Storage. *Adv. Funct. Mater.* **24**, 2630–2637 (2014).

60. Xia, X. *et al.* High-Quality Metal Oxide Core/Shell Nanowire Arrays on Conductive Substrates for Electrochemical Energy Storage. *ACS Nano* **6**, 5531–5538 (2012).

61. Agubra, V. A., Zuniga, L., Flores, D., Villareal, J. & Alcoutlabi, M. Composite Nanofibers as Advanced Materials for Li-ion, Li-O2 and Li-S Batteries. *Electrochimica Acta* **192**, 529–550 (2016).

APPENDICES

A. Summary of the conducted experiments in varying parameters

The table below illustrates the parameters investigated throughout the research. SEM images of the resulting materials were analyzed to determine the most suitable method, and further investigations were conducted based on the current method, which yielded the most homogeneous decoration throughout CC.

The chosen method may be considered optimal. A favorable environment for nanoparticle nucleation could result from pre-treatment of the carbon cloth. Additionally, maintaining the reaction vessel at lower temperatures for 48 hours may facilitate the growth of nanoparticles on the carbon cloth. Lastly, introducing manganese into the reaction mixture might potentially serve as a stabilizing agent for the structure at lower temperatures.

Table A. 1 Parameters for the hydrothermal synthesis of the MFS and MS on CC

Material	**Precursors**	**Solvent**	**Reaction Temperature (°C) / Time (s)**
MFS	2 mmol $FeCl_2.4H_2O$ + 2 mmol $MnCl_2.4H_2O$ + 4 mmol C_2H_5NS	30.0 mL isopropanol + 10.0 mL DIW	120 °C / 4 h
MFS	2 mmol $FeCl_2.4H_2O$ + 2 mmol $MnCl_2.4H_2O$ + 4 mmol C_2H_5NS	30.0 mL isopropanol + 10.0 mL DIW	150 °C / 4 h
MFS	2 mmol $FeCl_2.4H_2O$ + 2 mmol $MnCl_2.4H_2O$ + 4 mmol C_2H_5NS	30.0 mL isopropanol + 10.0 mL DIW	180 °C / 4 h
MFS	5 mmol $FeCl_2.4H_2O$ + 5 mmol $MnCl_2.4H_2O$ + 10 mmol C_2H_5NS	30.0 mL isopropanol + 10.0 mL DIW	120 °C / 4 h

Table A.1 (cont'd) Parameters for the hydrothermal synthesis of the MFS and MnS on CC

MFS	5 mmol $FeCl_2.4H_2O$ + 5 mmol $MnCl_2.4H_2O$ + 10 mmol C_2H_5NS	30.0 mL isopropanol + 10.0 mL DIW	150 °C / 4 h
MFS	5 mmol $FeCl_2.4H_2O$ + 5 mmol $MnCl_2.4H_2O$ + 10 mmol C_2H_5NS	30.0 mL isopropanol + 10.0 mL DIW	180 °C / 4 h
MFS	5 mmol $FeCl_2.4H_2O$ + 5 mmol $MnCl_2.4H_2O$ + 10 mmol C_2H_5NS	30.0 mL isopropanol + 10.0 mL DIW	120 °C / 12 h
MFS	5 mmol $FeCl_2.4H_2O$ + 5 mmol $MnCl_2.4H_2O$ + 10 mmol C_2H_5NS	30.0 mL isopropanol + 10.0 mL DIW	150 °C / 12 h
MFS	5 mmol $FeCl_2.4H_2O$ + 5 mmol $MnCl_2.4H_2O$ + 10 mmol C_2H_5NS	30.0 mL isopropanol + 10.0 mL DIW	180 °C / 12 h

Table A.1 (cont'd) Parameters for the hydrothermal synthesis of the MFS and MnS on CC

MFS	5 mmol $FeCl_2.4H_2O$ + 5 mmol $MnCl_2.4H_2O$ + 10 mmol C_2H_5NS	30.0 mL isopropanol + 10.0 mL DIW	120 °C / 24 h
MFS	5 mmol $FeCl_2.4H_2O$ + 5 mmol $MnCl_2.4H_2O$ + 10 mmol C_2H_5NS	30.0 mL isopropanol + 10.0 mL DIW	120 °C / 48 h
MFS	5 mmol $FeCl_2.4H_2O$ + 5 mmol $MnCl_2.4H_2O$ + 20 mmol C_2H_5NS	30.0 mL isopropanol + 10.0 mL DIW	120 °C / 48 h
MnS	5 mmol $MnCl_2.4H_2O$ + 10 mmol C_2H_5NS	30.0 mL isopropanol + 10.0 mL DIW	120 °C / 48 h
MnS	5 mmol $MnCl_2.4H_2O$ + 20 mmol C_2H_5NS	30.0 mL isopropanol + 10.0 mL DIW	120 °C / 48 h

Table A.1 (cont'd) Parameters for the hydrothermal synthesis of the MFS and MnS on CC

MFS	5 mmol $FeSO_4.7H_2O$ + 5 mmol $MnSO_4.7H_2O$ + 10 mmol C_2H_5NS	30.0 mL isopropanol + 10.0 mL DIW	120 °C / 12 h
MFS	5 mmol $FeSO_4.7H_2O$ + 5 mmol $MnSO_4.7H_2O$ + 10 mmol C_2H_5NS	30.0 mL isopropanol + 10.0 mL DIW	120 °C / 24 h
MFS	5 mmol $FeSO_4.7H_2O$ + 5 mmol $MnSO_4.7H_2O$ + 10 mmol C_2H_5NS	30.0 mL isopropanol + 10.0 mL DIW	120 °C / 48 h